Development of 3D Printed Materials for Rapid Fabrication of Pedestrian and Bicycle Infrastructure to Increase Mobility

FINAL PROJECT REPORT

by

Dawn Lehman
Mark Ganter
Hailey Stenslie
Jacob Roth
University of Washington

Katherine Kuder
Seattle University

Sponsorship
PacTrans, College of Engineering and Department of Civil and Environmental Engineering for

Pacific Northwest Transportation Consortium (PacTrans)
USDOT University Transportation Center for Federal Region
10 University of Washington
More Hall 112, Box 352700
Seattle, WA 98195-2700

In cooperation with U.S. Department of Transportation,
Office of the Assistant Secretary for Research and Technology (OST-R)

DISCLAIMER

The contents of this report reflect the views of the authors, who are responsible for the facts and the accuracy of the information presented herein. This document is disseminated under the sponsorship of the U.S. Department of Transportation's University Transportation Centers Program, in the interest of information exchange. The Pacific Northwest Transportation Consortium, the U.S. Government and matching sponsor assume no liability for the contents or use thereof.

TECHNICAL REPORT DOCUMENTATION PAGE

1. Report No.	**2. Government Accession No.** 01701488	**3. Recipient's Catalog No.**
4. Title and Subtitle Development of 3D Printed Materials for Rapid Fabrication of Pedestrian and Bicycle Infrastructure to Increase Mobility		**5. Report Date** October 2, 2020 **6. Performing Organization Code**
7. Author(s) and Affiliations Dawn Lehman, Professor, CEE, University of Washington 0000-0002-0823-1167 Mark Ganter, Professor, ME, University of Washington Katherine Kuder, Professor, CE, Seattle University Jacob Roth, Graduate Researcher, ME, University of Washington Hailey Stenslie, Undergraduate Researcher, CEE, UW		**8. Performing Organization Report No.** 2018-S-UW-3
9. Performing Organization Name and Address PacTrans Pacific Northwest Transportation Consortium University Transportation Center for Federal Region 10 University of Washington More Hall 112 Seattle, WA 98195-2700		**10. Work Unit No. (TRAIS)** **11. Contract or Grant No.** 69A3551747110
12. Sponsoring Organization Name and Address United States Department of Transportation Research and Innovative Technology Administration 1200 New Jersey Avenue, SE Washington, DC 20590		**13. Type of Report and Period Covered** Final Report. **14. Sponsoring Agency Code**
15. Supplementary Notes Report uploaded to: www.pactrans.org		

16. Abstract

Advancements in fabrication of manufacturing and medical systems are focusing on using computer-aided fabrication methods, also termed additive manufacturing or 3D printing. In civil engineering, we still rely on traditional methods of construction. Although some researchers and companies have investigated 3D printing of concrete, most have focused on form, not engineering properties. This research project will remedy that by investigating mix design methodologies, new extrusion techniques, and use of large-capacity testing equipment to advance the engineering of 3D printed concrete structures. This project first investigated previous work in this area. Next it studied extrudable and stable (in its fresh state) mix design(s). Finally, the researchers investigated the design of the extruder. This project was an initial investigation, with the ultimate objective of printing components for multi-modal concrete structures, such as pedestrian and bicycle bridges.

17. Key Words Three-Dimensional Printing; Concrete Mixes		**18. Distribution Statement**	
19. Security Classification (of this report) Unclassified.	**20. Security Classification (of this page)** Unclassified.	**21. No. of Pages** 54	**22. Price** N/A

Form DOT F 1700.7 (8-72) **Reproduction of completed page authorized.**

SI* (MODERN METRIC) CONVERSION FACTORS

APPROXIMATE CONVERSIONS TO SI UNITS				
Symbol	**When You Know**	**Multiply By**	**To Find**	**Symbol**
		LENGTH		
in	inches	25.4	millimeters	mm
ft	feet	0.305	meters	m
yd	yards	0.914	meters	m
mi	miles	1.61	kilometers	km
		AREA		
in^2	square inches	645.2	square millimeters	mm^2
ft^2	square feet	0.093	square meters	m^2
yd^2	square yard	0.836	square meters	m^2
ac	acres	0.405	hectares	ha
mi^2	square miles	2.59	square kilometers	km^2
		VOLUME		
fl oz	fluid ounces	29.57	milliliters	mL
gal	gallons	3.785	liters	L
ft^3	cubic feet	0.028	cubic meters	m^3
yd^3	cubic yards	0.765	cubic meters	m^3
	NOTE: volumes greater than 1000 L shall be shown in m^3			
		MASS		
oz	ounces	28.35	grams	g
lb	pounds	0.454	kilograms	kg
T	short tons (2000 lb)	0.907	megagrams (or "metric ton")	Mg (or "t")
		TEMPERATURE (exact degrees)		
°F	Fahrenheit	5 (F-32)/9 or (F-32)/1.8	Celsius	°C
		ILLUMINATION		
fc	foot-candles	10.76	lux	lx
fl	foot-Lamberts	3.426	candela/m^2	cd/m^2
		FORCE and PRESSURE or STRESS		
lbf	poundforce	4.45	newtons	N
lbf/in^2	poundforce per square inch	6.89	kilopascals	kPa

APPROXIMATE CONVERSIONS FROM SI UNITS				
Symbol	**When You Know**	**Multiply By**	**To Find**	**Symbol**
		LENGTH		
mm	millimeters	0.039	inches	in
m	meters	3.28	feet	ft
m	meters	1.09	yards	yd
km	kilometers	0.621	miles	mi
		AREA		
mm^2	square millimeters	0.0016	square inches	in^2
m^2	square meters	10.764	square feet	ft^2
m^2	square meters	1.195	square yards	yd^2
ha	hectares	2.47	acres	ac
km^2	square kilometers	0.386	square miles	mi^2
		VOLUME		
mL	milliliters	0.034	fluid ounces	fl oz
L	liters	0.264	gallons	gal
m^3	cubic meters	35.314	cubic feet	ft^3
m^3	cubic meters	1.307	cubic yards	yd^3
		MASS		
g	grams	0.035	ounces	oz
kg	kilograms	2.202	pounds	lb
Mg (or "t")	megagrams (or "metric ton")	1.103	short tons (2000 lb)	T
		TEMPERATURE (exact degrees)		
°C	Celsius	1.8C+32	Fahrenheit	°F
		ILLUMINATION		
lx	lux	0.0929	foot-candles	fc
cd/m^2	candela/m^2	0.2919	foot-Lamberts	fl
		FORCE and PRESSURE or STRESS		
N	newtons	0.225	poundforce	lbf
kPa	kilopascals	0.145	poundforce per square inch	lbf/in^2

*SI is the symbol for the International System of Units. Appropriate rounding should be made to comply with Section 4 of ASTM E380.
(Revised March 2003)

TABLE OF CONTENTS

Acknowledgments vii
Executive Summary ix
CHAPTER 1. Introduction 1
CHAPTER 2. Literature Review 3
2.1. 3D Printing and Extrusion of Concrete 3
2.2. 3D Printing and Concrete Material Properties 4
2.3. Fiber-Reinforced Cementitious Materials (FRCMs) 5
2.4. Time-Dependent Constitutive Modeling Methodology and Expressions 6
CHAPTER 3. Mix Design and Fresh-State Properties 9
3.1. Background 9
3.2. Development of Extrudable Mix Designs 10
3.3. Summary 17
CHAPTER 4. Piston-Driven Concrete Extruder for Additive Manufacturing 19
4.1. Extrusion Machinery 19
4.2 Initial Auger-Based Designs 20
4.3 Using the Extruder 29
CHAPTER 5. Summary and Future Directions 31
5.1. Summary of Research Findings 31
5.1.1 Literature Review 31
5.1.2 Printer Design 31
5.1.3 Mix Design 32
5.2. Future Work 33
CHAPTER 6. References 35
BIBLIOGRAPHY 37

List of Figures

Figure 1.1 Examples of concrete construction through 3D printing 2

Figure 2.1 Rapid deployment of materials through 3D printing 4
Figure 2.2 Effect of figures on tensile response 5
Figure 2.3 Time-dependent compressive (a) strength and (b) modulus for SCM concretes 6
Figure 2.4 Calculated k (efficiency) factors for different C/(S+A) values for t = (a) 7, (b) 14, (c) 28, and (d) 56 days, respectively 7
Figure 2.5 (a) Derived H(t) function and (b) Comparison of measured and calculated f'c values for all values to time 8

Figure 3.1 0.20 W/C ratio 12
Figure 3.2 0.24 W/C ratio 12
Figure 3.3 0.25 W/C ratio 12
Figure 3.4 Phase migration with sand trials 13
Figure 3.5 Effects of phase migration 13
Figure 3.6 0.20 W/C ratio with Walocel 14
Figure 3.7 0.25 W/C ratio with Walocel 14
Figure 3.8 0.30 W/C ratio with Walocel 14
Figure 3.9 0.35 W/C ratio with Walocel 14

Figure 4.1 SolidWorks rendering of the gantry machine; the stepper motors and drive mechanisms are not pictured 20
Figure 4.2 Hole-digging auger cementitious materials extruder 21
Figure 4.3 Screw pump cementitious materials extruder 21
Figure 4.4 Concept drawings for the sliding nut (left) and fixed nut (right) piston assembly concepts 23
Figure 4.5 Concept drawing for the removable cartridge system 21
Figure 4.6 Overview drawing of the extruder with notable features 25
Figure 4.7 Exploded view of the extruder, with parts numbered 26

List of Tables

Table 4.1 Cementitious mixture recipes, with components measured by dry weight 22
Table 4.2 List of assembly parts for the extruder 23

ACKNOWLEDGMENTS

The primary research funding was provided by Pactrans. Additional funding came from the UW College of Engineering (COE) and the Department of Civil and Environmental Engineering as part of the COE Strategic Research Initiative. All of the materials for the mix design were donated by Lafarge. The authors are grateful for this support.

EXECUTIVE SUMMARY

America's bridge infrastructure is in a state of severe deterioration, but the vast majority of these bridges are for vehicle transportation; with limited funds available to upgrade or replace bridges, there is almost no funding to support infrastructure construction for other transportation modes. The cost of constructing a bridge cannot solely be computed on the basis of material quantities alone; transportation of prefabricated structural components, costly equipment and labor, and impact on traffic flow have become larger and larger parts of the true construction cost. This research w the first phase in developing a new construction and structural solution for building pedestrian and bicycle bridges. It is well accepted that three-dimensional (3D) printing is going to revolutionize the construction industry. This project will expedite that revolution through the development of engineered concrete mix designs suitable for 3D printing. To date, research has not addressed the rheological properties of unhardened (green) concrete, which determine the printing process, or the structural properties of hardened, printed concrete, which determine design. The results of this research are a first step toward enabling the printing of pedestrian and bicycle bridges, which will save time and money and will bring new infrastructure to all communities.

The research program investigated new mix and printer designs for concrete. Whereas conventionally formed concrete structures rely on the formwork for strength and stability during the hardening process, components constructed with 3D printing must rely on their green strength (i.e., strength during the time when the concrete has set but has not appreciably hardened) and stiffness to resist instability, such as buckling and creep, during construction. Therefore, this research investigated 3D printing from the point of view of materials and structural engineering, rather than construction or form. The research findings included the following:

(1) Methylcellulose can provide the formed strength needed for printed concrete and should be included in the mix design.
(2) Superplasticizer can complement the methylcellulose to ensure the needed viscosity for printing.
(3) A screw-driven extruder capable of providing pressures exceeding 50 psi is needed to print these mix designs.

CHAPTER 1. INTRODUCTION

Most fields of engineering and medicine are seeing rapid transformation in the fabrication of customized components through additive manufacturing, also called three-dimensional (3D) printing. The same cannot be said for fields related to building construction, including structural materials and structurally engineered components. The construction industry is looking toward automated construction over the next decade, and 3D printing will be an important component of advancing construction in this manner. Figure 1.1 shows examples of non-engineered structures that have been built with 3D printing.

To meet this goal, engineered (rather than ad-hoc) materials are required. As discussed below, most 3D printed structures are not engineered and material properties are not specified. In addition, because 3D printed structures or structural components do not utilized formwork, fresh-state engineering properties—including strengths, moduli and layer-to-layer adhesion—play a critical role in their success.

During construction, the component must sustain its self-weight and be stable. To ensure structural stability, the engineer must understand the time-dependent engineering properties to simulate the response of the green-state component. There is also a substantial deviation from traditional precast or cast-in-place construction, which relies on formwork to sustain stability during construction. A third and important shortcoming of current printed concrete is its lack of tensile strength. Although some components have been printed with voids for placement of reinforcement (figure 1.1b), there have been no studies of fully printed structures with structural fibers to provide the tensile and shear strength of the printed materials.

a) Example of non-engineered 3D printed structure

b) Example of 3D printed "wall" with voids for reinforcing steel.

c) Modulated 3D printing

Figure 1.1 Examples of concrete construction through 3D printing

This project investigated several important engineering aspects of 3D printing through extrusion. The project studied previous work that has investigated 3D printing of concrete as well as new mix designs and extruder designs for 3D printing of engineered cementitious composites with and without fine aggregate. This report summarizes the research findings, including challenges and obstacles.

The report is organized as follows: Chapter 1 Introduction, Chapter 2 Literature Review, Chapter 3 Mix Design, Chapter 4 Design of the Printer, and Chapter 5 Summary, Findings and Future Work.

CHAPTER 2. LITERATURE REVIEW

2.1 3D Printing and Extrusion of Concrete

Three-dimensional (3D) printing of concrete usually uses power-based or extrusion-based techniques. Extrusion is a special manufacturing/construction technique that that has been used for decades for cementitious materials. In the extrusion process, a stiff, highly viscous dough is forced through a die of desired cross-section by either an auger or a ram. The dough must be soft enough to pass through the die, yet stiff enough to maintain its shape upon exit of the die. Consequently, low water/binder ratios and high volumes of fiber reinforcement can be used (up to 8 percent). High performance is achieved because of the high shear and compressive forces used during extrusion, which densify the matrix, improve the fiber-matrix bond, and align fibers in the direction of extrusion. The increased density of the matrix improves material durability because the ingress of water and other deleterious agents is more limited (Kuder and Shah 2010).

Research has indicated that extruded materials are dense, they possess a stronger fiber-matrix bond, and fibers are aligned in the direction of extrusion (Akkaya et al. 2000). A number of researchers have compared extruded and cast cementitious materials to observe the effects of processing. In general, extruded products have been found to have a higher strength, stiffness, and toughness than cast materials. However, because processing affects the fiber-matrix bond strengths and matrix compositions, the critical fiber length is different for cast and extruded composites and should be considered (Shao et al. 2001, Peled and Shah 2003).

There is great interest in using 3D printing for structural applications (e.g., building or bridge construction). However, to date, most investigations have focused on architectural form or building construction (examples shown in figures 2.1 a and b, respectively). For example, patented work by Rael (UC Regents 2014) and Sabin et al. (2014) focused on the use of 3D printing for form. Figure 2.1a shows an example of powder-based 3D printing used to construct a 9-foot tower. Others have begun to focus on the required fresh-state material properties and computer automation required to achieve construction at a member or structure scale, as demonstrated by extrusion- based 3D printing (e.g., Lim et al. 2012). Although these endeavors have made significant advancements in their respective fields (i.e., architecture and construction), they have not focused on the rheological, processing, and

engineering properties needed to meet structural demands. Without this information, it is not possible to apply this construction advancement to the rapid prototyping or construction of mid- to high-rise structures.

(a) 3D printing for Form

(b) Concrete-only 3D printing

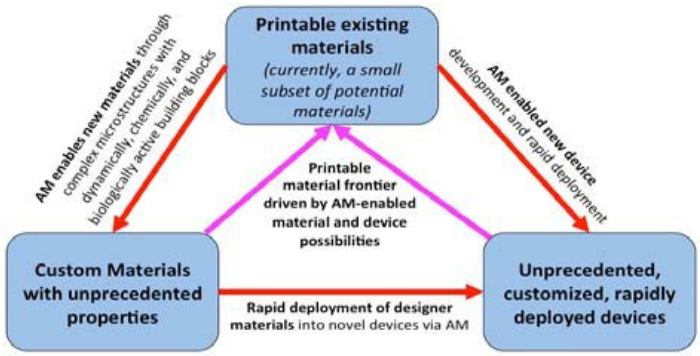

(c) Methodology for AM^2 (Ganter 2016)

Figure 2.1 Rapid deployment of materials through 3D printing

2.2 3D Printing and Concrete Material Properties

Materials-focused investigations into 3D printing extrusion processes have been very limited. Perrot and colleagues (Perrot et. al 2015). looked at the role of structural buildup in cement paste by using a "squeeze test." By using parameters from this fresh-state test, they developed a methodology to relate vertical stresses to plastic deformation and yield stress. Their final model showed the relationship between yield stress and time. This research was limited to a cement paste sample without any fibers.

Le et al. (2012) extruded high-performance, fiber-reinforced cementitious materials (HPFRCM) with 12-mm-long polypropylene microfibers by using a 9-mm nozzle and printing in a layered process. In addition to mechanical properties, voids were measured with image analysis (Le et al. 2012). The authors found a strong correlation between printing time gap and layer bond strength. Fiber alignment was not measured; however, the strength of the extruded HPFRCC clearly increased in comparison to a cast sample. The authors attributed this to fiber alignment. An increase in voids was seen with the printed samples.

Principal investigators Lehman and Ganter are participating in a UW-sponsored strategic research initiative (SRI) to investigate rapid deployment of materials through additive

manufacturing. The effort is entitled the "Advanced Materials and Additive Manufacturing (AM^2) Initiative"; the objectives and approaches are depicted in figure 2.1c, which also indicates the flow of information. (Note that the project is providing matching money.) This seed funding has been used to establish collaborative activities that cut across departments and colleges, including (wo workshops and student-led seminars to leverage AM/3D printing to deliver innovations with designer materials. The specific objectives are to 1) expand the spectrum of materials used, 2) enhance and innovate material design, 3) implement design and analysis tools that support 3D printing capabilities for spatially controlled properties, and 4) and develop next-generation 3D printing systems that support localized addition of a broad spectrum of designer materials. This research project will be integrated into the larger SRI and will specifically address the National Academy of Engineering's grand challenge to "Restore and Improve Urban Infrastructure" (also a grand challenge of the UW College of Engineering) through the rapid prototyping and demand- specific design of high performing, sustainable building materials.

2.3 Fiber-Reinforced Cementitious Materials (FRCMs)

Cementitious composites are typically characterized as brittle, with a low tensile strength and strain capacity. Fibers are incorporated into cementitious matrices to overcome this weakness, producing materials with increased tensile strength, ductility and toughness and improved durability. The efficacy of the fiber reinforcement is dependent upon many factors, including the properties of the matrix as well as the fiber geometry, size, type, volume, dispersion and orientation (Balaguru and Shah 1992).

The general tensile behavior of cementitious composites is shown in figure 2.2. Plain, unreinforced cementitious materials exhibit a strain-softening response with low tensile strength and ductility. Conventional fiber-reinforced composites (FRC) reinforced with a volume of fibers between 0.5 and 2 percent, also have a strain-softening response but demonstrate an increase in post-peak ductility. With HPFRCC, there is an increase in the elastic limit (defined as the point at which the first macrocrack is formed;before that, microcracking dictates performance), followed by a strain-hardening response that results when multiple cracks form but do not widen. Finally, strain softening is seen as cracks widen. Researchers have demonstrated that this high performance can

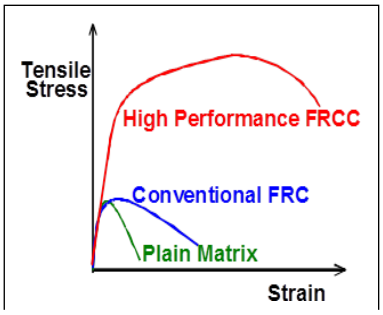

Figure 2.2 Effect of fibers on tensile response

be achieved in a variety of ways, including by using micromechanical modeling (Li and Wang 2001), tailored fiber geometries (Naaman 2003), and advanced processing techniques (Shao et al. 1993, Peled et al. 2000, Peled and Shah 2003, Mobasher and Pivacek 1998).

2.4 Time-Dependent Constitutive Modeling Methodology and Expressions

Conventional construction utilizes concrete forms. These forms (typically wood or steel) make up a significant part of the total cost of constructing a concrete building. Printing fiber-reinforced cementitious materials (FRCMs) relies on green-state properties for strength and stability because these structures/structural components are not formed or molded. Whereas formed reinforced concrete construction is well known and the forms are designed to provide strength and stability to the concrete in its green state, the stability and sufficient strength of printed FRCM during construction is not known, and each project will present unique geometry and loading. Therefore, it is critical to investigate the response of the printed FRCM components during the construction process through advanced FEM analysis. It is critical to establish the properties of the 3D printed material (both green and hardened).

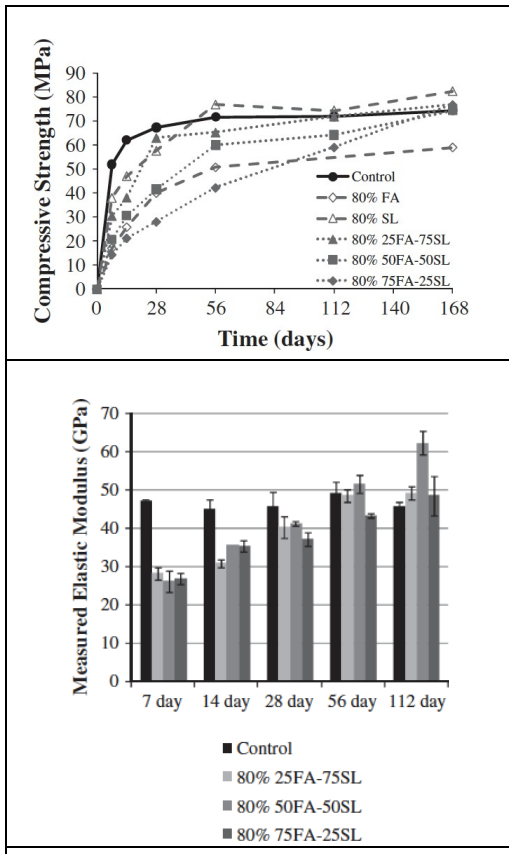

Figure 2.3: Time-dependent compressive (a) strength and (b) modulus for SCM concretes

It is well established that cement-only or primarily cement with partial supplementary cementing materials (SCM) mixes (a fly ash percentage of 35 or less) develop the vast majority of their hardened engineering properties within seven days. For high-cement replacement mixes (above 60 percent), the cure time is elongated, and time-dependent concrete properties are needed to ensure stability during construction. This dependency is shown in figure 2.3a, which shows different strength versus time curves for SCM concretes with the same cement replacement ratio (80 percent) but different mix designs, and figure 2.3b, which shows the dependency of modulus on time. In addition, a base mix with 100 percent cement is also shown. Clearly strength depends

on the mix design here, characterized by the ratio of CaO to $SiO_2 + Al_2O_2$, abbreviated as C/(S+A). The same is true for the materials considered here, with time-dependent strength being more important because it is critical for stability during construction.

This and other research by the principal investigators (Kuder et al. 2012, Hannesson et al. 2012, and Chen et al. 2017) on time-dependent modeling of SCM concrete has resulted in three new models for compressive strength, modulus, and creep. Modeling of time-dependent compressive strength has been achieved by introducing time-dependent coefficients to a modified Bolomey equation. The research process is as follows:

1. Gather test results (figure 2.3a and b show typical test results for compressive strength and modulus).
2. Derive values for time-dependent coefficients. Figure 2.4 shows kP, the equivalent cement content for the SCM, for 7, 14, 28, and 56 days, respectively, as a function of C/S+A.

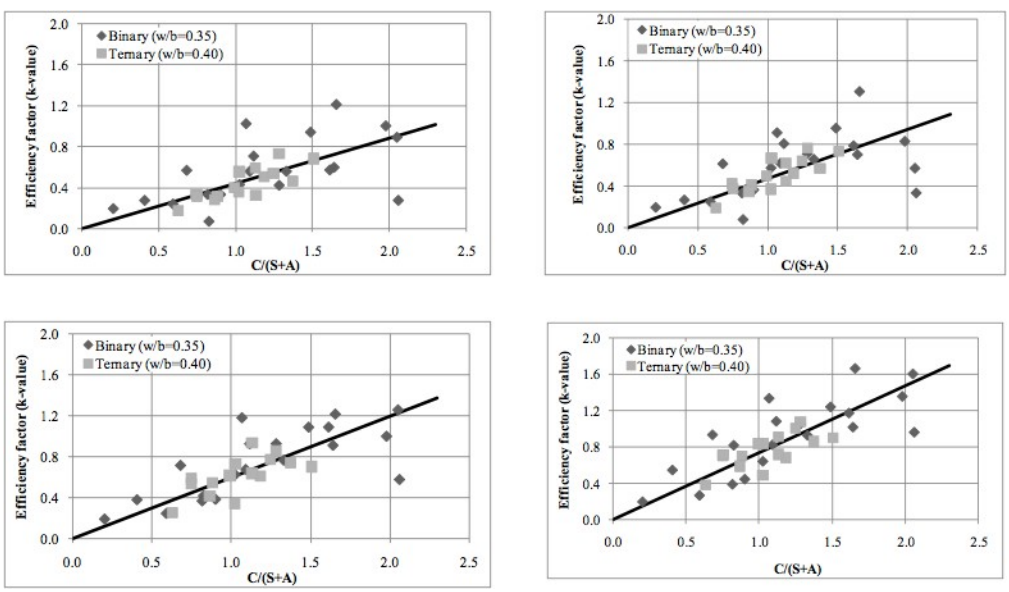

Figure 2.4: Calculated k (efficiency) factors for different C/(S+A) values for t = (a) 7, (b) 14, (c) 28 and (d) 56 days, respectively.

Figure 2.5a shows the derived expression for H(t) using the previous test results. Note that the uncertainty in each value of H at time t_i is from the different values of C/(S+A). Therefore, one can use the derived expression for H(t) shown on the graph or derive H(t) for the mix designs of interest. Figure 2.5b shows the results (measured on the x axis and calculated

using the modified Bolomey equation and the derived function for H(t) on the y axis) for the PIs' tests as well as 50 other test programs. As evident by the plot, the results are sufficiently accurate for use in design. This work provided one of the first equations for time-dependent compressive strength for SCM concretes. The elastic modulus of the material can be computed at any time during curing by using the EuroCode equation. Similar work has been done to develop creep expressions that account for the time-dependent modulus (Chen et al. 2017).

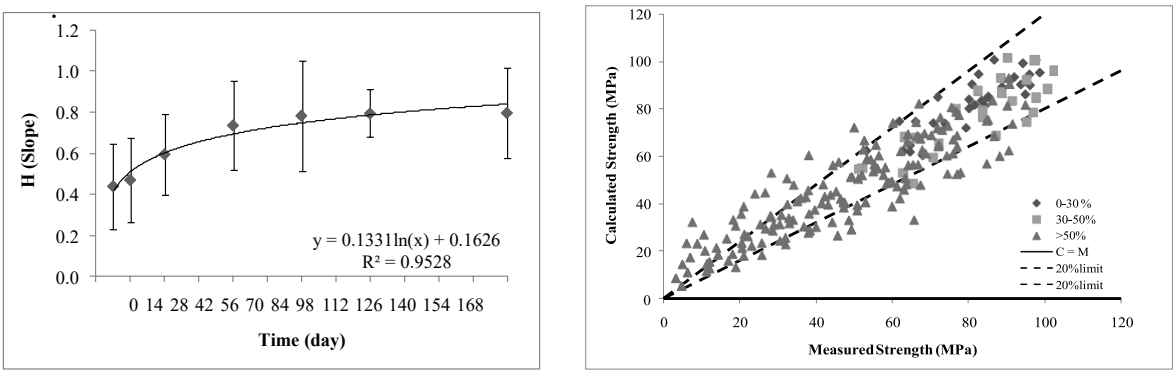

Figure 2.5: (a) Derived H(t) function and (b) comparison of measured and calculated f'_c values for all values of time (Kuder et al. 2012)

This approach was used in this research program, in which Task 3 measured the engineering properties of FRCMs and Task 4 established a time-dependent expression for use in investigating the response of the 3D printed structural components/structures.

Using that work as a basis for this research, the team decided to focus on two aspects of the proposed project: (1) an open source mix design that would provide the fresh-state properties needed to simultaneously print the concrete and have enough strength to sustain its own weight and that of the layers above, and (2) design of an extruder for a larger scale (24- by 24-inch build space). The first topic is addressed in Chapter 3. The second topic is addressed in Chapter 4.

CHAPTER 3. MIX DESIGN AND FRESH-STATE PROPERTIES

Advancements in the fabrication of manufacturing and medical systems have focused on using computer-aided fabrication methods, also called additive manufacturing or 3D printing. In contrast, civil engineering still relies on traditional methods of construction. Although researchers and companies are investigating 3D printing of concrete, most have focused on form, not on engineering properties. This research project was begun to remedy that by investigating mix design methodologies, new extrusion techniques, and use of large-capacity testing equipment to advance the engineering of 3D printed concrete structures. This research task investigated extrudable and stable (fresh state) mix design(s); a new protocol was developed to test the engineering properties, including stiffness, strength of the extruded material, and multi-layer adhesion and deformation.

3.1 Background

Throughout the digital age, technology and automation have increasingly replaced the need for manual labor. The construction industry should be no different. Processes are being streamlined through increases in technology available. Current concrete construction is focused on completing each project as quickly and efficiently as possible. The construction process involves building formwork for the concrete to be poured into, then waiting until the concrete has set to remove the formwork. The major cost of construction involving concrete is the formwork, which can account for more than 60% of the cost. Typically, structures are designed to have identical members, making the formwork reusable. This does eliminate material costs for the project, as formwork is typically made of wood. However, it does little for the labor costs associated with building, disassembling, and reassembling the formwork, which in turn increase a project's cost. The concepts is that 3D printed concrete would decrease construction costs because it does not require formwork,. Current 3D printing technology works with materials such as plastics that are heated to become malleable enough to extrude and then harden almost instantly after being printed. Some have begun to print with clays and ceramics, constructing complex pottery. 3D printing of concrete is expected to build on this technology.

This task focused on developing a printable mix design. This mix needed to be easily repeatable for simplicity in construction. Developing the mix design included several trials with different admixtures to produce a mix that would have minimal slump and would not deform

under the weight of subsequent layers. The fresh-state properties of the concrete were especially important because of this. The initial strength of the concrete needed to be determined to establish the number of layers the base could support without visible deformation. As concrete cures it gains strength, gaining full strength in the first 28 days. The material properties for the new mix would need to be established for this method to be used in construction today. Cylinders and beams would be printed to determine these material properties. They would be cured and tested at time intervals of 1 hour, 12 hours, 24 hours, 3 days, 7 days, and 28 days.

3.2 Development of Extrudable Mix Designs

The following method was used to design prototype mixes to evaluate their "printability." The following properties of the mix designs were evaluated: (i) consistency, (ii) post-extrusion shape, and (iii) ability to support subsequent layers without excessive deformations. The following steps were used to establish and evaluate the mixes.

1. A target water to cement ratio (W/C) was determined. The mix included cement and water. W/C ratios of 0.20, 0.24, 0.25, 0.27, 0.28, and 0.30 were tested. After these W/C ratios had been tested, a mix containing 0.25 was used in the majority of the mix design. Further testing (see step 2) determined that a W/C ratio of 0.30 should be used to develop a printable mix design.
2. Sand was added into the mix after the target W/C ratio had been determined. The sand was tested to determine moisture content and absorption percentage. These parameters changed the amount of water in the mix and were essential in determining a standard for 3D printing of concrete mixes. Adding sand into the mix caused it to become extremely viscous and not able to be extruded. To mitigate this problem, the W/C ratio was increased until the mix was extrudable. This W/C ratio was determined to be 0.30 for the addition of sand and any future mixes.
3. Once an extrudable mix containing sand had been developed, Walocel was added. Walocel is a chemical, like the one used in plaster, that reacts with water and helps the concrete hold its shape. This admixture is very important for mitigating layer deformation and phase migration. 1 percent of the weight of the mix was used to determine the amount of Walocel to add. This was then decreased to 0.05 percent of the total weight, as the mix was determined to be too viscous to be printable.
4. Several super plasticizers were tested to determine which type of base would perform

best with our current mix design. Rheobuild 3000 was determined to be the most applicable super plasticizer. Typically, super plasticizers are added to a concrete mix to decrease the W/C ratio and make the mix less viscous. However, this is not the case with the addition of Walocel. The super plasticizer was added to the current mix design to help with mitigate phase migration during extrusion. The company that creates Rheouild 3000 suggested that 0.6 to 2 percent by weight of cement be added to the mix. A range of percentages was tested until 0.6 percent was chosen for use. This created the least viscous mix while helping with phase migration.

5. To evaluate the mixes, hand extrusion was accomplished with an electric caulking gun. This simple extrusion process permitted investigation of the shape and strength of the extruded layers. This initial phase identified several issues. When a bead was extruded, the concrete had a tendency to slump and deform under its self-weight and the weight of the layers placed on top. The mix also had a problem with phase migration. This problem became so prevalent during extrusion that some mix designs could not be extruded. Both of these issues had to be resolved before printing could occur.

Next the mix design was evaluated qualitatively. Consistency, appearance, viscosity, texture, and visible deformation were examined to determine which mix was most suitable for 3D printing.

The mix design with a 0.2 W/C ratio was thick and crumbly and very difficult to extrude; the sample experienced phase migration to the point at which it could not be extruded. Figure 3.1 shows the extruded mix containing water and cement. The mix appeared very dry but did hold its shape under self-weight. Figure 3.2 shows the extrusion with a W/C ratio of 0.24. This mix was more malleable and easier to extrude but still appeared a little dry. When sand was added to the mixture it stiffened; therefore, a wetter mix was better to start with. Figure 3.3 shows a W/C ratio of 0.25. This mixture was less stable but extremely easy to extrude. The characteristics of this mix seemed most suitable to continue with as more variables were added into the mixture. The mixtures below only contained water and cement, and these trials were conducted to determine a starting point for further mix development.

Figure 3.1 0.20 W/C ratio

Figure 3.2 0.24 W/C ratio

Figure 3.3 0.25 W/C ratio

A moisture content test and absorption test were both performed on the sand to determine the amount of water that would need to be added into the mix. The mix was then extrudable with both the Walocel and Rheobuild 3000. Sand was then added into the mixture to create higher mix stability and increase compressive strength. Several different W/C ratios were tested, and all experienced phase migration, as shown in figures 3.4 and 3.5. Phase migration could not be controlled by only adjusting the W/C ratio; therefore Walocel was added to mitigate this problem.

Figure 3.4 Phase migration with sand trials

Figure 3.5 Effects of phase migration

Walocel was added to help with phase migration and create an extrudable mix. Adding 1 percent Walocel, by weight of cement had adverse effects on viscosity, making the mix thicker and affecting the extrudability of the mixture. Increasing the W/C ratio to 0.30 and decreasing the Walocel content to 0.05 percent created a consistency and viscosity that appeared to be suitable for printing. Figure 3.6 show a mixture with a W/C ratio of 0.20; even though the mixture was extrudable, it was very dry and appeared to be cracking. The mixture in figure 3.7 had a W/C ratio of 0.25 and appeared suitable for extrusion; however, the mixture was still among the more viscous of concrete mixes for 3D printing. The mixture in figure 3.8 had a W/C ratio of 0.30; this mixture was less viscous than the previous attempted mixture. It appeared to have a suitable consistency, viscosity, and could support its self-weight as well as subsequent layers. Figure 3.9 shows a mixture with a W/C ratio of 0.35, which was much less viscous than that of the previous trial with W/C ratio of 0.30. There was also significant deformation of the layers when subsequent layers were placed on top, making it least sufficient for 3D printing.

Figure 3.6 0.20 W/C ratio with Walocel

Figure 3.7 0.25 W/C ratio with Walocel

Figure 3.8 0.30 W/C ratio with Walocel

Figure 3.9 0.35 W/C ratio with Walocel

Initially the mixes are extruded from an electric caulking gun, which works the same way a piston extrusion system would. The mix was pushed out rather than driven out as with an auger system. Using a piston system is more beneficial because the concrete is compressed during extrusion. This action works in parallel with the concrete's strengths. Using an auger system works against concrete strengths by the concrete it as it extrudes. This shearing works to create excess pressure that the auger must overcome before the system can extrude the mix. If this pressure becomes too high, the motor driving the auger begins to skip and cannot extrude the cement.

The mix was developed by first looking at a mortar mixture containing only water and cement, then addeing sand and admixtures to further curate it to become printable. The W/C ratio was changed numerous times to determine the differences that occurred when other components were added to the mixture. A W/C ratio of 0.30 was determined to be most effective when all the components were added into the mixture. In developing the mixture, it was important to start with a base line technique that is currently used in concrete construction. American Concrete

Institute (ACI) concrete proportioning standards were used in creating the weights of each component. For the admixture content, standards presented by industry experts or manufacturers were used to determine weight.

Once each component had been added to the mixture and tested for extrudability, it was essential to define the process of mixing the concrete. Creating a process for mixing the concrete would create less variability in the quality of the mix produced. This process could then be repeated and refined as testing proceeded. The concrete was mixed in an electric concrete mixer that resembled a Kitchen Aid mixer. The solid materials were all be mixed together first to create the most homogeneous mixture possible. To facilitate the homogeneity of the mixture, the cement and Walocel were weighed out together, and the sand was weighed out separately. The ACI suggests that all aggregates be first mixed together then the cement be added on top of the mixed aggregate. To follow this procedure, the sand was first placed in the mixing bowl with the cement placed on top of it, and it was then mixed together for 60 seconds. The water and Rheobuild 3000 were then weighed out and added to the mixer after 60 seconds while the mixer was continuously running. The mix was then mixed for 90 seconds and evaluated qualitatively. This resulted in a relatively homogenous mix for printing.

Consistency, color, and viscosity were observed when the concrete mixture was removed from the bowl. Tests were conducted for up to an hour after the mix had been removed from the mixer. After this hour the mixture was too viscous to print.

The concrete mixes were evaluated for many qualitative properties, such as consistency, viscosity, and color. Initial properties were determined by using a starting mix, then were determined for each new parameter introduced (e.g., w/c ratio, admixture, sand volume). Each new mix design was calculated, mixed, and then evaluated for these properties. Color was evaluated with pictures, while consistency and viscosity were measured by the designer's judgment. The mix was then extruded from the caulking gun first, and if it proved extrudable, it was extruded with the initial 3D printer auger system. If the mix failed to be extruded in either step, the mode of failure was determined and the mix was redesigned accordingly. Phase migration, interlayer deformation, and failure to be extruded were all considered different modes of failure and were evaluated differently.

Interlayer deformation (slump) is a major concern for 3D printed structures. To achieve a structurally sound member, the layers must be uniform and not splay excessively. Sodium CMC

was the first carboxymethylcellulose substance to be added to the cement mixture. This helped with the layer slumping but did not help with phase migration. The addition of this required an increase in the W/C ratio and caused phase migration to worsen as the trials continued. Phase migration is a process in which liquid is essentially squeezed out of a material. In this case the water separating from the mixture caused a decrease in the W/C ratio, making the mix very viscous and unable to be extruded. Phase migration can be seen in figure 3.4, and its results are shown in figure 3.5.

Walocel is also a methylcellulose material, and it was tested to better combat phase migration with layer slump. Initially a mix of 1 percent Walocel by weight was added to the concrete mixture. After this mixture had been printed, the Walocel was decreased to 0.05 percent by weight of the whole mix. The concrete mixture with the Walocel became sticky (tacky), and the viscosity decreased significantly. The decrease in viscosity was as expected; however, the sticky (tacky) nature of the cement mix was not. This characteristic was encouraging in looking at the layer to layer adhesion. The mix with the Walocel tended to clump together more like a clay, was light grey in color, and appeared shiny. The developed mix had a repeatable consistency and appearance that should be modeled for consistency. With the addition of the Walocel, the phase migration problems had been virtually eliminated, and the mix held its shape under self-weight and the weight of subsequent layers. Many trials were conducted with a W/C ratio of 0.3 and 0.5 percent Walocel. The W/C ratio had to be increased because of the reduction in viscosity the Walocel caused.

A W/C ratio of 0.30 was printable and allowed multiple layers to be stacked without significant deformation in the layers.

Along with the addition of the Walocel, a super plasticizer was used to help reduce the W/C ratio and further prevent any phase migration that might occur with large-scale printing. Initially, Rheobiuld 3000 was used before the addition of methylcellulose. This helped reduce the W/C ratio from 0.3 to 0.255, with a dosage of 20 cc/kg. If the W/C ratio was decreased any further, the mix could not be extruded from the caulking gun.

To enhance the printability, Fritzpak Supercizer 5 was used. Fritzpak is a Naphthalenesulfonic acid based super plasticizer. Initially, addition of the super plasticizer increased the stiffness of the mix, which reduced its extrudability. The motor on the auger would move in an irregular pattern (“skip”) when the recommended dosage was used. Fritzpak

recommends 1.75 pounds per yard of concrete. After the mix was determined to be unviable for printing, the Supercizer 5 was removed from the mix. (More information on this is provided in Chapter 4.)

The superplasticizer Rheobuild 3000 was then added, starting with 2 percent by weight of the cement. When the Rheobuild was added to the mix, it became very stiff and crumbly. The amount of Rheobuild was reduced to 0.06 percent by weight of cement in the mix. The addition of the Rheobuild affected the viscosity of the mixture, making it slightly stiffer but still workable. It had been previously observed that the super plasticizer could negatively affect the mixture if too much was added or if the W/C ratio was decreased too much. To counteract these issues, the W/C ratio was set at 0.30. The current mix using 0.06 percent Rheobuild 3000 was extrudable, and no phase migration occurred during the printing process.

3.3 Summary

On the basis of these small-scale experiments, the final recommendations for the mix design were as follows:

- a W/C ratio of 0.3
- 0.06 percent super plasticizer (here Rheobuild 3000 was used)
- 0.5 percent methylcellulose (here Walocel was used).

This information alone provides a good starting point for a mix design for 3D printing. The next chapter discusses investigation of the design of the extruder for the concrete printer and the trials of printing this mix.

CHAPTER 4. PISTON-DRIVEN CONCRETE EXTRUDER FOR ADDITIVE MANUFACTURING

In the additive manufacturing (AM) field, "material extrusion" refers to the process of building an object by using a nozzle that squirts out material and can be moved around in three dimensions.

Material extrusion processes build up a three-dimensional object layer by layer, forming each layer by moving this nozzle around in a plane and squirting out material in the shape of the object. Each new layer sticks to the previous layer below it and provides a building platform for the future layer above it. Material extrusion is currently the most popular technology for additively manufacturing small plastic objects, and the basic concept of additive manufacturing with cementitious material extrusion is to scale this process up to the size of buildings and use wet cementitious material instead of hot thermoplastic.

4.1 Extrusion Machinery

To print with cementitious material extrusion requires both an extruder to squeeze out the cementitious material and a robotic arm or gantry system. These two pieces must be integrated from a design perspective, but conceptually they are independent. this research focused on both the extrusion machinery and extrusion process.

Cementitious material in its wet, freshly mixed state is generally a viscous, semi-fluid mixture that is reasonably modeled as a Bingham plastic. Squeezing a viscous fluid out of a small nozzle opening for additive manufacturing requires a pump, and re two basic types have been used in the literature: axial flow pumps (generally helical augers) and positive-displacement pumps (generally pistons). Screw pump extruders use a rotating helical blade to create a pressure differential, while positive displacement systems trap a fixed amount of material and push it along. Positive-displacement systems have the advantage of directly linking the flow rate of the (largely incompressible) wet mixture to the motion of the pump's parts, and thus to the motion of the motor driving the system. This means the flow rate through a positive-displacement system can be easily controlled with just motor position. In contrast, the flow rate through an axial flow pump depends on controlling the pressure. Some researchers have used off-the-shelf concrete pumps of both types in cementitious material AM research.

The cementitious material AM systems presented in the literature have also differed in how they have deliver wet material to the extruder. In some systems, the wet cementitious mix is fluid enough to be pumped from a stationary hopper to a moving extruder with an ordinary concrete pump. In others, the mix is loaded into a hopper that moves around with the extruder, and in the simplest research designs the extruder has carried around only a small amount of wet material.

Over the course of about a year, the research team built a meter-scale, three-axis computerized numerical control (CNC) gantry system for use as a cementitious materials 3D printer (figure 4.1). The full design details of this machine are outside the scope of this report, but in summary, it was designed to lift an extruder with a mass of up to 40kg and position it to within ±1cm in a roughly one-cubic-meter build volume. It was driven by five NEMA23 stepper motors. The team also designed an electrical and control system for it, which drioe each of the NEMA23 steppers through a stand-alone stepper driver at 36 V and was also capable of driving a single extruder stepper motor through a much larger (up to 7.2 A capacity) stand-alone stepper driver at 60 V. All of these drivers were controlled via a USB motion card and the MACH3 software running on a small Windows computer.

Figure 4.1: SolidWorks rendering of the gantry machine; the stepper motors and drive mechanisms are not pictured.

4.2. Initial Auger-Based Designs

The first research into cementitious material AM at the University of Washington was a Mechanical Engineering Department senior capstone project that developed an axial flow-type

extruder based around a commonly available 3-in.-diameter hole-digging auger and a 1.5-in.-diameter nozzle opening (figure 4.2). This first extruder could only extrude a cementitious material without sand.

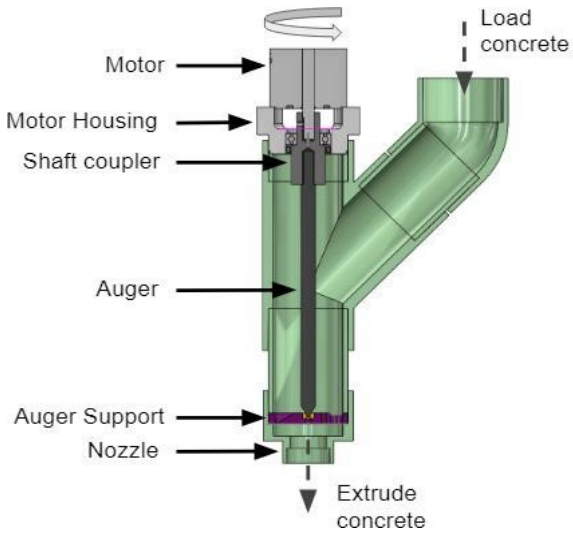

Figure 4.2: Hole-digging auger cementitious materials extruder

To address issues with extrusion, the research team designed a screw pump extruder (figure 4.3). This design used the same large stepper motor and 1–in. nozzle opening, but a smaller 2-in. auger as the motive screw, so that the extruder would work with a much smaller volume of wet mix at a time. However, this smaller extruder exhibited the same failure modes. The motor housing and the body of the extruder were held together only by a friction fit, severely limiting the amount of torque the motor could exert on the wet mix before it caused the two pieces to rotate relative to each other and come loose.

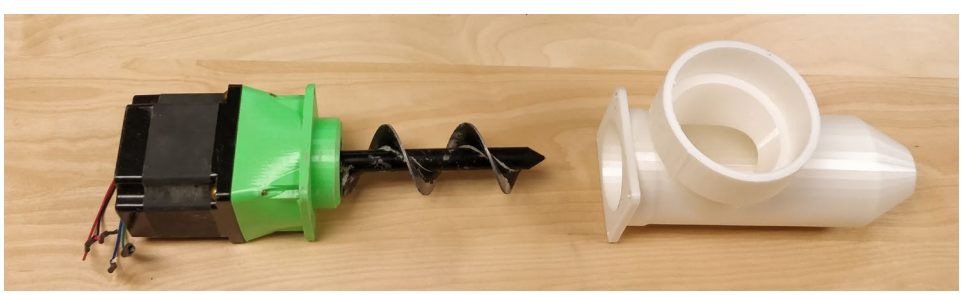

Figure 4.3: Screw pump cementitious materials extruder

The work described in Chapter 3 noted that the caulk gun was able to easily extrude some of the same types of cement mixtures that had failed to print in the screw pump extruder. Therefore, the team investigated whether an extruder system built with a piston or other type of positive- displacement pump might work better than the screw pump systems.

The first aspect investigated was the force exerted by an effective piston extruder. This was determined experimentally by plugging a 1-in.-diameter nozzle opening on the end of a 2-in.-diameter pipe, filling it with one of Hailey's mixtures, and then inserting a piston into the pipe and adding weights to the top until the piston was under enough pressure to extrude the cementitious mixture. The team determined that a basic cement mixture with sand (table 4.1, mix 1) required 46 psi to extrude from a 2-in. cylinder to a 1-in. nozzle,

Table 4.1: Cementitious mixture recipes, with components measured by dry weight.

Mix No.	Mix name	Water (wt. %)	Cement (wt. %)	Sand (wt.%)	Walocel (wt. %)	Rheobuild (wt. %)
1	Piston test (Low-sand)	19.1	63.8	17.0	0.0258	0.060
2	Piston test (Full-sand)	8.85	29.5	61.6	0.0148	0

On the basis of these initial investigations, the following objectives were set for the printer design:

1. Positive-displacement design (figure 4.4)
2. Minimum extrusion pressure of 100 psi
3. The three-axis CNC gantry powered entirely by stepper motors. (If there had been additional time and resources, hydraulic or AC motors might have been tested as prime movers for their mechanisms, but the researchers wanted to design something that could run directly off the stepper motor drivers that had already been set up.)
4. Portable (ease of use and transport)
5. Rapid loading and unloading process and easy-to-clean moving parts.

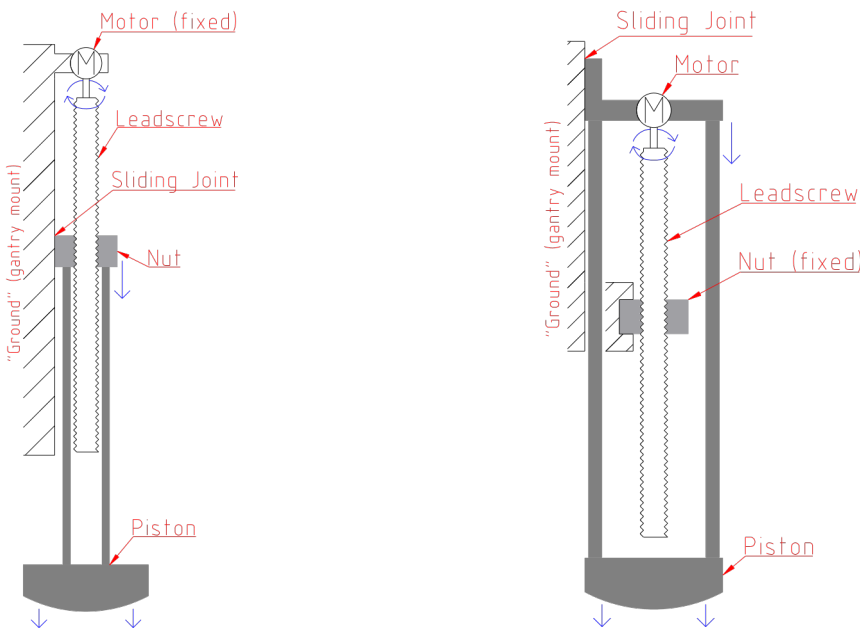

Figure 4.4: Concept drawings for the sliding nut (left) and fixed nut (right) piston assembly concepts.

Figure 4.4. shows two concepts for the piston assembly. In both cases, a motor would rotate a leadscrew in a nut, and the fact that the nut would be constrained to not rotate relative to the motor would force it to translate, pushing the piston. The crucial difference between these two was which part of the assembly was held fixed (relative to the gantry) and which part the piston attached to. With the goal of exerting 100 psi on the wet cementitious material using a piston and the prime mover of a stepper motor, a mechanical linkage was needed to connect the two. The goal of converting motor rotation to low speed, high force translation (with noise and mediocre mechanical efficiency being acceptable) meant that a leadscrew and nut system was the best solution. Driving a piston with such a system would require a leadscrew, a nut, and a mechanism to force them to rotate relative to each other (without some other part of the assembly rotating instead).

To streamline the experience of loading the extruder and to prevent messy and difficult clean-ups (Section 1.3.5), the researchers envisioned a cartridge-based loading and unloading system that would use removable cementitious material cartridges made of PVC pipe and 3D printed plastic (figure 4.5). The concept of the design was as follows: the extruder piston would slide into the cartridge and force the cementitious material out a plastic nozzle that was

permanently attached to the other end of the cartridge. The only part of the extruder other than the cartridge that would touch wet cementitious material would therefore be the end of the piston, and therefore the piston heads would be fabricated from 3D-printed plastic and easy to replace. The result was an extruder system in which all the parts that were expected to get very messy (from the concrete) could be easily removed and either cleaned or cheaply replaced.

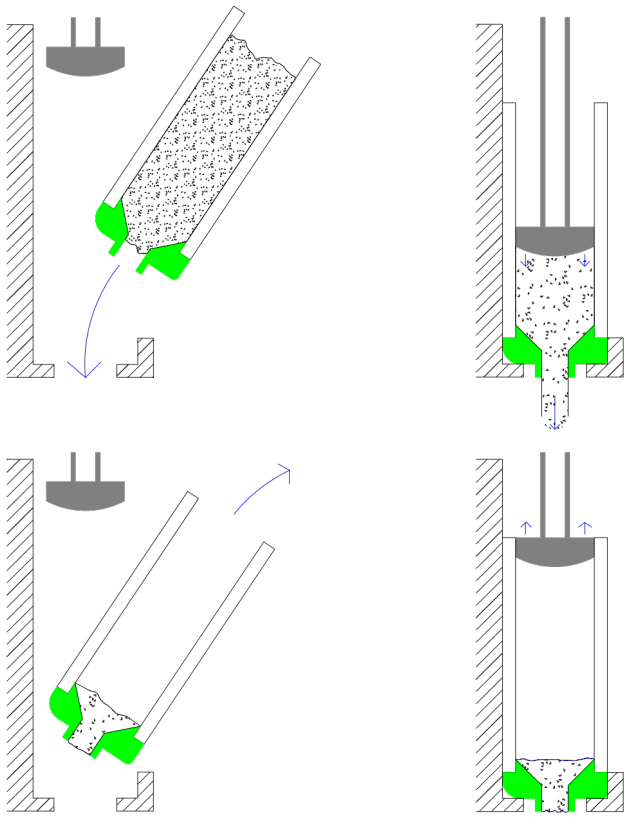

Figure 4.5: Concept drawing for the removable cartridge system.
Clockwise from top left: 1) The operator "rocks" the cartridge full of wet cementitious material into the extruder. 2) The cartridge is "locked" firmly in place by the descending piston during the extrusion stroke. 3) After reaching the bottom, the piston returns to its starting position, unlocking the cartridge. 4) The operator removes the almost- empty cartridge. Spent cartridges can be manually refilled through the top.

The extruder design is shown in figure 4.6. It consisted of an aluminum box called the receiver (Assembly Part #1, see figure 4.7 and table 4.2), with a fixed ACME nut (#20) underneath the upper lid (#2). The primary moving part was a slide consisting of an aluminum plate (#3) on the top and a 3D printed piston holder (#26) on the bottom, connected by a pair of linear motion shafts (#7) that rode in small linear sleeve bearings (#14). A leadscrew (#21), driven by a stepper motor (#29) by way of a gear reduction (#5 and #22), forced the slide to

move up or down through a set of thrust bearings (#1719). Cartridges of cementitious materials (#4 and #24, glued together) were inserted through the side of the receiver and optionally secured with a locking pin (#25). Finally, a detachable piston (#27) moved with the slide and forced cementitious material out the cartridge's integrated nozzle (interior of #24, not shown).

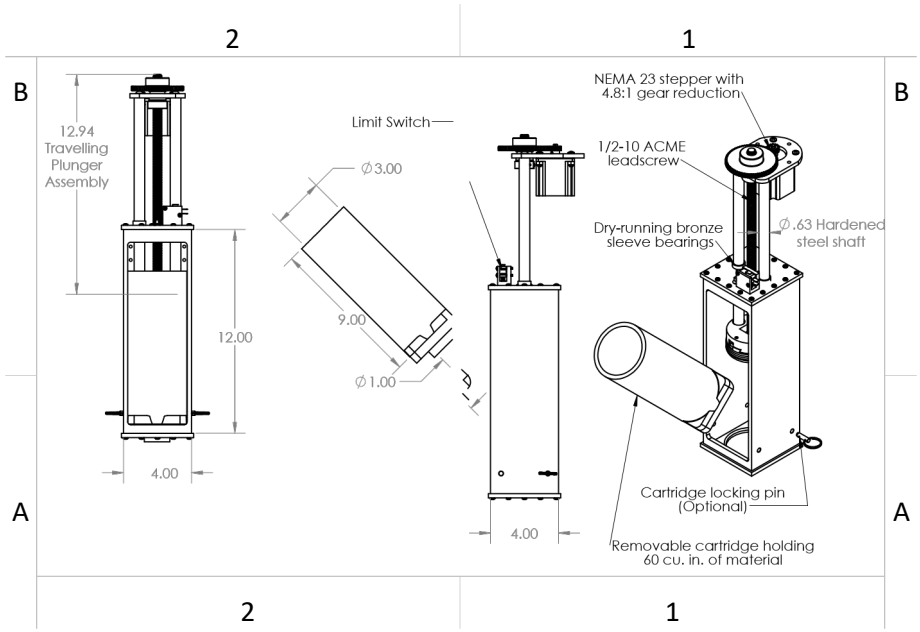

Figure 4.6: Overview drawing of the extruder with notable features.

Like most additive manufacturing extruders, this design was intended to be controlled by CNC software (such as MACH3) as a generic CNC axis. Therefore, it featured a limit switch mounted on the receiver (#16) that was actuated by a screw mounted on the piston slide (#28) when the piston slide reached its uppermost position. This allowed the controller to home the extruder as it would home any other axis.

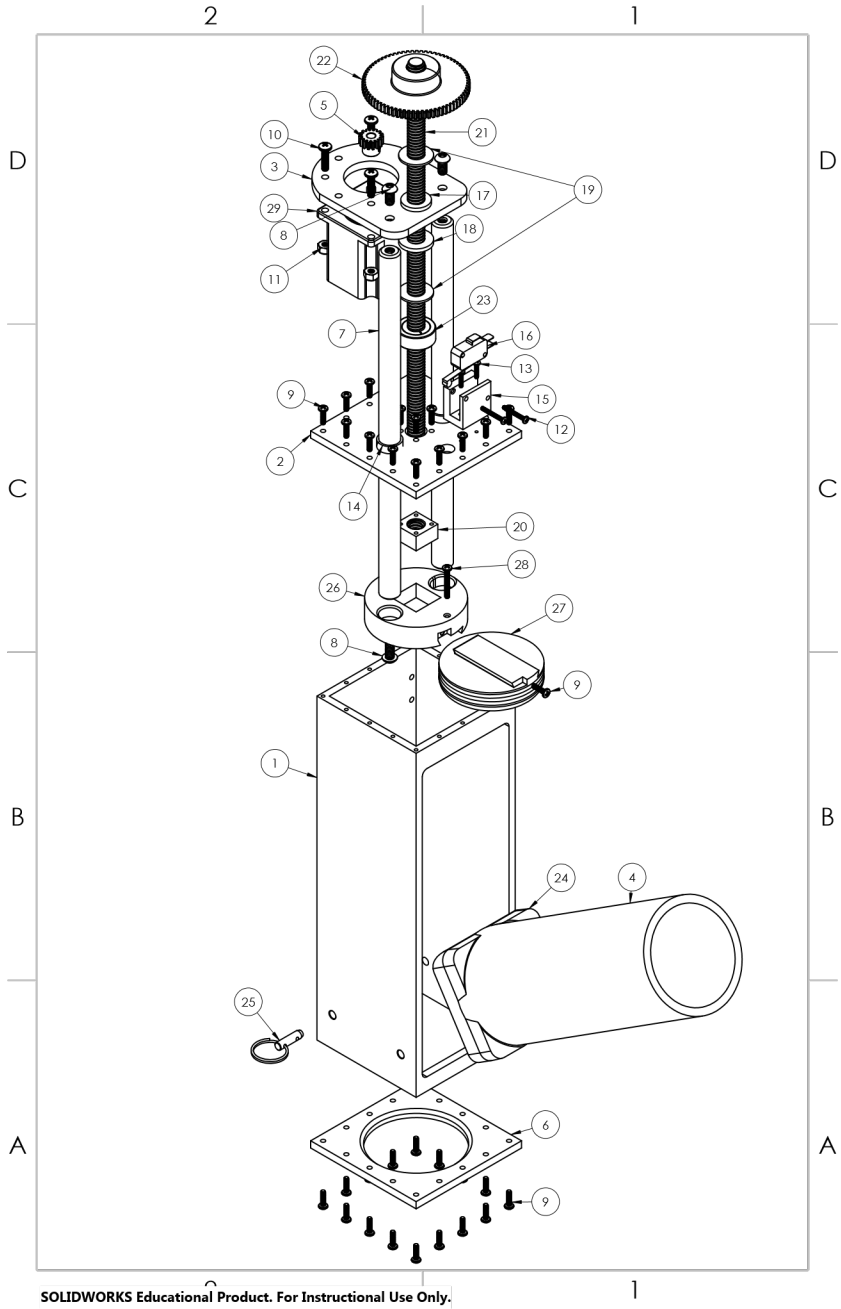

Figure 4.7: Exploded view of the extruder, with parts numbered (see table 4.2, leftmost column).

Table 4.2: List of assembly parts for the extruder

Assembly Part No.	External Part No. / Name	Qty.	File Name in Assembly
1	Receiver-Short-Cartridge	1	Reciever-Short-Cartridge
2	Cap-Fixed-Nut	1	Cap-Fixed-Nut
3	Moving-Top-Plate	1	Moving-Top-Plate
4	PVC Tube	1	PVCTube
5	6867K557	1	6867K557_MTL GEAR--14-.5 DEG PRESSURE ANGLE
6	Bottom-Plate-Simple	1	Bottom-Plate-Simple
7	6649K7	2	6649K700_HARDENED PRECISION STEEL SHAFT
8	92949A537	3	92949A537_Quarter-20-Screw-Half-Inch-Long
9	91772A148	37	Half-Inch-6-32-Screw
10	94836A363	4	ThreeQuarter-Inch-10-32-Screw
11	91831A411	4	10-32-Nylock
12	91772A114	2	Seven-Eighths-Inch-4-40-Screw
13	91772A110	2	Half-Inch-4-40-Screw
14	9368T64	2	9368T640_HIGH-TEMPERATURE DRY-RUNNING SLEEVE BEARING
15	LimitSwitchHolder	1	LimitSwitchHolder
16	Micro Switch.step	1	Micro Switch.step
17	9440T21	1	9440T210_HIGH-TEMP DRY-RUNNING FLANGED SLEEVE BEARING
18	7447K7	1	7447K700_HIGH-TEMPERATURE DRY-RUNNING THRUST BEARING
19	7447K5	2	7447K500_HIGH-TEMPERATURE DRY-RUNNING THRUST BEARING
20	95270A114	1	95270A114_ModifiedWithHoles_BRASS GENERAL PURPOSE ACME SQUARE NUT
21	98935A911	1	98935A911_CutDown_ASTM A108 STEEL ACME LEAD SCREW
22	6325K67	1	6325K670_MTL GEAR--14-.5 DEG PRESSURE ANGLE
23	2228N11	1	2228N110_CLAMPING ACME LEAD SCREW COLLAR
24	RockInNozzle	1	RockInNozzle
25	98320A124	2	98320A124_ZINC-PLATED STEEL QUICK-RELEASE PIN
26	PistonHolderDovetailed	1	PistonHolderDovetailed
27	Printed-Piston-Dovetail	1	Printed-Piston-Dovetail
28	91772A153	1	One-Inch-6-32-Screw
29	6627T53	1	6627T530_POSITION-CONTROL DC MOTOR

The basic design pattern of a linear axis with two parallel sliders riding in two parallel bearings is known to be troublesome because it is overly constrained and thus liable to bind.

However, the proposed design had two key features intended to mitigate this risk. The first was that the distance between the two guide rods would not actually be constrained at the bottom end, because the piston holder (#26) would only be screwed into one of the rods and would allow the other rod to move slightly closer or farther away from its partner. The second was that the piston sliding in the cartridge would act as another "semi-bearing," preventing the large angular deflections associated with slide binding but having enough overall movement to prevent binding.

The extruder was powered by a standard NEMA23 stepper motor with a nominal 2.5 A current rating (assembly part #29, see table 4.2), which was advertised on McMaster-Carr as producing 8.75 in.- lbs of torque at starting and 1.06 in.-lb. of torque at a top speed of 600 rpm. This motor drove the main gear through a 15:72 gear reduction. Analysis of this system indicated that the motor was capable of pressures of approximately 65 psi. Although this fell short of the 100 psi target, the research team moved forward with this design because it was within the budget.

The extruder was fabricated by students using a 3D printer. Building the extruder required access to a milling machine, drill press, arbor press, basic hand tools, and a way of completing one weld on carbon steel (between the leadscrew and the main gear, see figure 4.7, #21 and #22). The 29 distinct parts in the assembly (table 4.2) fit into five categories:

1. Parts bought from McMaster-Carr and used as-is:
   (#5, #7-14,#17-19, #22-23, #25, #28-29)
2. Parts bought from McMaster-Carr and modified slightly:
   - Leadscrew (#21) cut down to appropriate length
   - Square ACME nut (#20) drilled and tapped for machine screws
3. Parts machined from aluminum plate and square tube stock (#1-3, #6) or 3-in. Schedule 40 PVC pipe (#4)
4. Parts additively manufactured on an ordinary 3D printer, using a SunLuPLA Plus filament (#15, #24, #26-27)
5. An ordinary limit switch (#16).

Machining the receiver (#1) was by far the most difficult and time-consuming part of manufacturing the extruder. This part required machining on all six sides, including the top and bottom, which were difficult to reach and impossible to tap with the milling machines available

in the Mechanical Engineering prototype shop. To create the 32 tapped holes on the top and bottom of the receiver, it was necessary to use the mill to drill 1/16-in. pilot holes in the right spots, then use a drill press to enlarge each one to .1065 in., then tap each one to #6-32 thread by hand. In hindsight, 16 of those tapped holes (and their matching through-holes on the plate) could hypothetically have been avoided by welding the bottom plate (#6) in place instead of using screws. (Welding the top plate (#2) was not an option because it would have made replacing the linear bearings (#14) almost impossible.)

These linear bearings also made the top plate somewhat awkward to manufacture; it was critical to mill out the bearing holes in the plate, remove the plate from the mill, arbor press the bearings into place (causing them to shrink slightly), and then return the plate to the mill and use a 5/8-in. reamer to ream out the bearings to exactly 5/8 in.

In contrast to these machining operations, the use of plastic 3D printing to create the piston (#27) and nozzle-containing cartridge base (#24) would made these parts basically painless to manufacture and should allow for easy experimentation with different geometries if desired. This would serve the overall goal of creating an extruder for future research in AM with cementitious materials.

4.3 Using the Extruder

The following outlines the use of the extruder.

1. Set-up and configuration. The extruder was bolted to the gantry system and the stepper motor was wired into the large stepper driver. The motion card then exposed the extruder motor to the MACH3 software as a fourth axis (the A axis). The steps per millimeter were tuned in the software until the position of the piston could be controlled with G-Code.
2. Load cell tests. A 1000-pound (1-kip) capacity load cell was used to measure the force that the extruder's piston could actually exert at zero speed. The force was measured at motor stall with the piston pressed up against the load cell's plate and the motor powered from the 60-V power supply at peak current limits from 2.8 A (the controller's minimum) to 4.9 A (well in excess of the stepper's nominal 2.5 A rating). At 2.8 A (the stepper driver's lowest setting and very close to the stepper's nominal rating), the extruder exerted 353 pounds of force, somewhat short of the predicted 484 pounds using theoretical analysis. To

achieve the predicted force, the motor current was increased to 4.2 A. It is suspected that the difference between the theoretical and actual forces was due to friction. The measurements indicated that 353 pounds of force corresponded to 50 psi of pressure on the cementitious material, which should still be adequate for extruding some cementitious mixtures. If higher pressures are needed, the stepper should be run at a higher current, adding heatsinks and fans as necessary to prevent overheating.

Because of the timing of the printer assembly and mix design, the team was unable to test the mix in the printer. However, there are two aspects of the printer design that are unique. One is the removable cartridge design, which will facilitate testing a wide variety of cementitious material mixes and nozzle geometries. The low cost and ease of manufacture of these removable cartridges also means that having a particular mixture fail to extrude and then setting up the cartridge will not be a major loss.

The second is the positive-displacement design, which will allow direct connection to link motor steps to millimeters of extruded "filament" in exactly the way that off-the-shelf 3D printing slicer software (such as Slic3r or Ultimaker Cura) expects. This should make it possible for researchers to additively manufacture cementitious materials without having to write G-Code by hand or develop a custom slicer, saving them considerable development time.

The one caveat with using this extruder with existing 3D printing workflows is that the piston, unlike a conventional plastic additive manufacturing extruder, can extrude only a limited amount of material before it must be reloaded. It should be possible to work around this issue by writing a postprocessing script that searches the G-Code intended for the printer for any travel moves that would take the extruder beyond its limit of travel, takes note of the current A-coordinate at that point, then prepends G-Code to do the following:

1. Back up the piston to its uppermost position.
2. Pause the program for the operator. The operator will then remove the spent cementitious material cartridge and insert a new one. The operator will then resume the program.
3. Push the piston down a few centimeters to "prime" the extruder.
4. Reset the A-coordinate to what it was before.

CHAPTER 5. SUMMARY AND FUTURE DIRECTIONS

5.1 Summary of Research Findings

The following summarizes the findings of each aspect of the research project.

5.1.1 Literature Review

The research team investigated previous work conducted on printing concrete. The primary findings were as follows:

1. Most research conducted on 3D printing of concrete has been conducted in Europe.
2. Most 3D printing of concrete has focused on architectural form or other non-engineered components.
3. Fine aggregate (sand) is almost never included in the mix designs; most printing is of a cementitious mortar not concrete.
4. Although publications have discussed the fresh state materials of 3D printed mixes, they have not proved the mix design.
5. Most printers are designed and fabricated by companies, and therefore the printer design is proprietary.

The conclusion was that although the literature review was useful, it left the team with very little information about previous work because most was proprietary and, therefore, did not provide much guidance. This proved to be a distinct disadvantage, especially for such a short timeline.

5.1.2 Printer Design

1. The research team included Mark Ganter, a professor of Mechanical Engineering. Mark has been involved in 3D printing since 2009. He has built a series of printers with different build scales. The printer for this project used a three-axis gantry (called an MPCNC).
2. The printer built had a print area of 24 x 24. This would allow printing of cylinders, prisms, and panels/slabs
3. The team spent most of their resources on the extruder design. 3D printing uses either extrusion or powder printing. Most cementitious materials (including clay) use extrusion-based printing. The team investigated the size and shape of the extruded region. The extruder was fabricated with a 3D printer in the Mechanical Engineering 3D printing laboratory that is directed by Professor Ganter. The research was

conducted by Professor Ganter's ME research student, Jacob Roth. In the end, the team chose a rectangular extruded shape, which provided benefit for layer stability and printing rectangular components (most concrete components are rectangular).

4. Several issues with the mechanical engineering of the printer were explored, including (1) pump pressure, (2) motor properties, (3) rotating vs sliding extrusion piston, (4) bearing design, and (5) stiffness of the gantry.
5. In the end, the printer did print concrete but not until after the project had been completed, and the concrete that was printed did not have fine aggregate (sand). The team realized that designing a large-scale 3D printer was outside of the research budget. The team plans to write an STF proposal to buy a 3D printer from a company.

5.1.3 Mix Design

1. The mix design was overseen by Professor Lehman and her colleague Professor Kuder. Professor Kuder has expertise in concrete materials, complementing Professor Lehman's expertise in structural engineering. Professors Kuder and Lehman have collaborated successfully on other research projects.
2. The mix design research was conducted by CEE undergraduate research student Hailey Stenslie.
3. For 3D printing, there are mix design complexities that are unique to this construction method. Most importantly, the mix must be extrudable but also able to hold its own shape after printing and able to withstand the weight of layers that will be above the printed layer. To achieve this, the team used methylcellulose admixture in the mix design. By using hand-extruded layers, the team was able to extrude the mix and meet these requirements. This was a successful aspect of the project. An evaluation was conducted to compare different water-to-cement ratios and different amounts of methylcellulose
4. Another complexity is the addition of sand. As noted in the literature review, sand has not been included in the vast majority of mix designs for 3D printing. The team very much wanted to explore the addition of sand, as it is a necessary component for concrete. The researchers found that sand decreased the extrudability of the mix substantially. There was significant phase migration with the sand; this was somewhat mitigated with the methylcellulose.

5. The team was unable to test any hardened specimens, so the focus was solely on the mix design.

5.2 Future Work

Several aspects of the printer design need to be improved before it can be used for additive manufacturing. First the extrusion pressure should be increased to 70 to 100 psi to consistently extrude a variety of cementitious mixtures that include fine aggregate. The simplicity of the stepper-motor driven design should make it easy to use this extruder with different types of printing robots and electronic control schemes as those become available to UW researchers. Additionally, the integration of the extrusion nozzle into the removable cartridge, rather than the body of the extruder, should make it fairly easy to experiment with different nozzle sizes and geometries. Other improvements would be to use a different system for raising and lowering the piston, specifically to shorten the load path and minimize sliding and vibrating of the piston slide while still preventing the motion system from binding.

Alternatively, the team is considering purchasing a commercial concrete printer. If this purchase is successful, the team will focus on the mix design, including fibers in the mix, as was in the original proposal, as well as determine the hardened engineering properties of the concrete.

CHAPTER 6. REFERENCES

Akkaya, Y., A. Peled, and S.P. Shah, (2000) "Parameters Related to Fiber Length and Processing in Cementitious Composites." *Materials and Structures*. 33(232): pp. 515-524.

Balaguru, P. and Shah, S.P. *Fiber Reinforced Cement Composites*, McGraw- Hill, (1992), pp. 530.

Chen, J., Kuder, K., Lehman D., Roeder C., and Lowes L. (2017) "Creep Modeling of Concretes with High Volumes of Supplementary Cementitious Materials and its Application to Concrete- Filled Tubes", Materials and Structures, 50(1) February 2017.

Ganter, M. "Advanced Materials and Additive Manufacturing Initiative (AM^2) http://blogs.uw.edu/am2i/ (2017)

Hannesson, G., Kuder, K., Shogren, R., and Lehman, D. "The Influence of High Volume of Fly Ash and Slag on the Compressive Strength of Self-Consolidating Concrete," *Construction and Building Materials*, 30(3), 2012, pp. 161-168.

Kuder, K.G. and Shah, S.P. (2010) "Processing of High-Performance Fiber-Reinforced Cement-Based Composites." *Construction and Building Materials: Special Issue on Inorganic-Bonded Fiber Composites*, 24(2), pp. 181-186.

Kuder, K., Lehman, D., Berman, J. Hannesson, G., and Shogren, R. (2012) "Mechanical Properties of Self Consolidating Concrete Blended with High Volumes of Fly Ash and Slag," *Construction and Building Materials*, 34, pp. 285-295.

Le. T, Austin, S.A., Lim, S., Buswell, R.A., Law, R., Gibb, A.G.F., Thorpe, T. (2012) "Hardened properties of high-performance printing concrete" Cement and Concrete Research 42 (2012) 558–566.

Li, V.C. and S. Wang, (2001) "Tensile Strain-Hardening Behavior of Polyvinyl Alcohol Engineered Cementitious Composites (PVA-ECC)." *ACI Materials Journal*, 98(6): p. 483-492.

Lim, S, Buswell, T. Austin, S, Gibb, A., and Thorpe, T. (2012) "Developments in construction-scale additive manufacturing processes" Automation in Construction 21 (2012) 262–268.

Mobasher, B. and A. Pivacek, (1998) "A Filament Winding Technique for Manufacturing Cement Based Cross-Ply Laminates." *Cement and Concrete Composites*. 20(5): p. 405-415.

Naaman, A.E., (2003) "Engineered Steel Fibers with Optimal Properties for Reinforcement of Cement Composites." *Journal of Advanced Concrete Technology*.1(3): p. 241-252.

Peled, A., M. Cyr, and S.P. Shah, (2000) "High Content of Fly Ash (Class F) in Extruded Cementitious Composites." *ACI Materials Journal*. 97(5): p. 509-517.

Peled, A. and S.P. Shah, (2003) "Processing Effects in Cementitious Composites: Extrusion and Casting." *Journal of Materials in Civil Engineering*, 15(2): p. 192-199.

Perrot, A., Rangeard, D. and Pierre, A. (2015) “Structural built-up of cement-based materials used for 3D printing.” Materials and Structures, DOI 10.1617/s11527-015-0571-0

Sabin J., Miller M., Cassab N., and L. (2014) 3D Printing and Additive Manufacturing. June 2014, 1(2): 78-84. doi:10.1089/3dp.2014.0012.

Shao, Y., Z. Li, and S.P. Shah, (1993) "Matrix Cracking and Interface Debonding in Fiber-Reinforced Cement-Matrix Composites." *Advanced Cement-Based Materials*, 1(2): p. 55-66.

Shao, Y., Qiu, J. and Shah, S.P. (2001) “Microstructure of Extruded Cement-Bonded Fiberboard,”*Cement and Concrete Research*, 31(8), pp. 1153-1161.

UC Regents (2014), US 20140252672 A1. Patent. N.d. Print.

BIBLIOGRAPHY

Bakri, A. M. M. Al, Kamarudin, H., Bnhussain, M., Nizar, I. K., Rafiza, A. R., and Zarina, Y. (2012). "The Processing, Characterization, and Properties of Fly Ash Based Geopolymer Concrete," *Rev. Advanced Materials Science*, 30, pp. 90–97.

Bagley, E.B., "End Correction in the Capillary Flow of Polyethylene." *Journal of Applied Physics*, 1957. 28: pp. 624-627.

Buswell A. "3D Printing Using Concrete Extrusion: A Roadmap for Research". In: *Cement and Concrete Research*. SI : Digital Concrete 2018 112 pp. 37–49. October 2018. issn: 0008-8846. doi: 10.1016/j. cemconres.2018.05.006. url: http://www.sciencedirect.com/ science/article/pii/S0008884617311924

Emerging Objects (2016) http://www.emergingobjects.com/projects/bloom-2/

Hertzman 2018, "Countdown to Human-Free Construction in Less Than 10 Years" https://www.forconstructionpros.com/profit-matters/article/20987766/countdown-to-humanfree-construction-in-less-than-10-years)

Jastrzebski, Z.D., "Entrance Effects and Wall Effects in an Extrusion Rheometer During the Flow of Concentrated Suspensions." *Industrial and Engineering Chemistry - Fundamentals*, 1967. 6(4): pp. 445-453.

Khan, A.U., B.J. Briscoe, and P.F. Luckham, "Evaluation of Slip on Capillary Extrusion of Ceramic Pastes." *Journal of European Ceramic Society*, 2001. 21(4): p. 483-491.

Kuder, K. and Shah, S.P. (2007) "Rheology of Extruded Cement-Based Composites." *ACI Materials Journal*, 104(3), pp. 283-290.

Kuder, K., Ozyurt, N., Mu, E., & Shah, S. (2007). Rheology of Fiber-Reinforced Cement Systems Using a Custom-Built Rheometer. In *Brittle Matrix Composites 8* (pp. 431-439). Elsevier Ltd. DOI: 10.1533/9780857093080.431

Lin, T., Jia, D., He, P., Wang, M., and Liang, D. (2008). "Effects of fiber length on mechanical properties and fracture behavior of short carbon fiber reinforced geopolymer matrix composites," *Materials Science and Technology A*, 497, pp. 181–185.

Lu, B. "A Systematical Review of 3D Printable Cementitious Materials". In: *Construction and Building Materials* 207 (May 2019), pp. 477–490. issn: 09500618.

Majidi, B. (2009). "Geopolymer Technology: From Fundamentals to Advanced Applications : a Review," *Materials Technology*, 24(2), pp. 79–87.

Malaeb (2015) "3D Concrete Printing: Machine and Mix Design". In: *International Journal of Civil Engineering and Technology* 6 (June 2015), pp. 14–22.

Rahul, A."3D Printable Concrete: Mixture Design and Test Methods". In: *Cement and Concrete*

Composites 97 (Mar. 2019), pp. 13–23. issn: 09589465.

Russel H. and Graybeal, B. (2013) "Ultra-High Performance Concrete: A State-of-the-Art Report for the Bridge Community", Office of Infrastructure Research & Development, Federal Highway Administration, Publication No. FHWA-HRT-13-060, June 2013.

Soltan, D.G. and Victor C. Li. "A Self-Reinforced Cementitious Composite for Building-Scale 3D Printing". In: *Cement and Concrete Composites* 90 (July 2018), pp. 1–13. issn: 09589465.

Suuronen, J.P, Kallonen A., Eik M., Puttonen J., Serimaa R. and Herrmann, H. (2013) "Analysis of short fibres orientation in steel fibre-reinforced concrete (SFRC) by X-ray tomography", J Mater Sci (2013) 48:1358–1367, DOI 10.1007/s10853-012-6882-4.

Yunsheng, Z., S. Wei, and Z. Li, (2006) "Impact Behavior and Microstructural Characteristics of PVA Fiber Reinforced Fly Ash-Geopolymer Boards Prepared by Extrusion Technique." *Journal of Materials Science*, 41(10): pp. 2787-2794.

Zellars, R. 2015 "Ryan Zellars shares designs for impressive mostly 3D printed RepRap CNC machine", 3ders.org 3D printer and 3D printing news, July 2015. https://www.3ders.org/articles/20150728-ryan-zellars-shares-designs-for-impressive-mostly- 3d-printed-reprap-cnc-machine.html

Zhou, X. and Z. Li, "Characterizing Rheology of Fresh Short Fiber Reinforced Cementitious Composites Through Capillary Extrusion." *Journal of Materials in Civil Engineering*, 2005. 17(1): pp. 28-35.